A regional susceptibility assessment for shallow landslides in central Taiwan

Lin, Meei-Ling, Chen, Yen-Chen, and Liu, Te-Chu

Department of Civil Engineering, National Taiwan University, Taipei, Taiwan

linml@ntu.edu.tw

Abstract

The frequency and extent of landslide hazard might increase due to the increasing trend of severe rainfall events caused by climate change as suggested by many researchers. Among different types of landslide, the shallow landslides occurred frequently and extensively, and often triggered debris flow. In this research, the susceptibility analysis was conducted for debris flow basins in a study area in central Taiwan. Inventory of the shallow landslide was screened and edited considering the corresponding grid size of analysis unit. The causal factors were selected and tested for independency and significance, and the discriminant analysis was conducted for assessment of shallow landslide susceptibility. The constructed susceptibility model was validated with a separate group of data, and both the fitting and validation groups provided consistent accuracy and good results. The backward prediction was conducted using the historical inventory data, and a comparable accuracy was achieved, which suggested the robustness of the susceptibility model. Finally, a regional susceptibility map was established accordingly.

1 INTRODUCTION

Taiwan situates at the convergence zone of tectonic plates, and the geological condition is fragile with more than 70 % of the area considered as the mountain area. Landslide hazard was often triggered by earthquakes and/or heavy rainfalls in Taiwan. The frequency and extent of landslide hazard might increase due to the increasing trend of severe rainfall events (Lin, et al., 2017b). Among different types of landslides, the shallow landslides occurred frequently and covered extensive region. The shallow landslides in small basin could have triggered debris flows (Harp, et al., 2006, Lin, et.al., 2014), which have been the cases and one of the major hazards in Taiwan. The development of a shallow landslide susceptibility map provides reference for mitigation strategy not only for the shallow landslide mitigation, but also for the debris flow mitigation policy.

In this research, the susceptibility analysis was conducted for debris flow basins in a study area in central Taiwan. Inventory of all types of landslides was collected and checked for analysis. The shallow landslide inventory was then screened and edited considering the corresponding grid size of analysis unit. The causal factors were selected and tested for independency and significance, and the discriminant analysis was conducted for assessment of shallow landslide susceptibility. The constructed susceptibility model was then validated with a separate group of data. The backward prediction was conducted using the historical inventory data, and a regional susceptibility map was established accordingly.

2 STUDY AREA

The study area locates in central Taiwan, which includes mainly the Xinsher District, and parts of the Taiping and Dongshi Districts, Taichung City, and Juolan Town, Miaoli County, with Tachia River flowing through from east to west as shown in Figure 1. The geological map of the study area is shown in Figure 2. The study area locates in the Western Foothill Geological Zone in Taiwan, where the geological formations are mainly composed of un-metamorphic sedimentary rocks of sandstone, siltstone, shale, and sandstone/shale interlayer of the Miocene epoch. The geological formations in the study area includes Kueichulin Formation, which is massive sandstone, siltstone, and sandstone intercalated alternations of

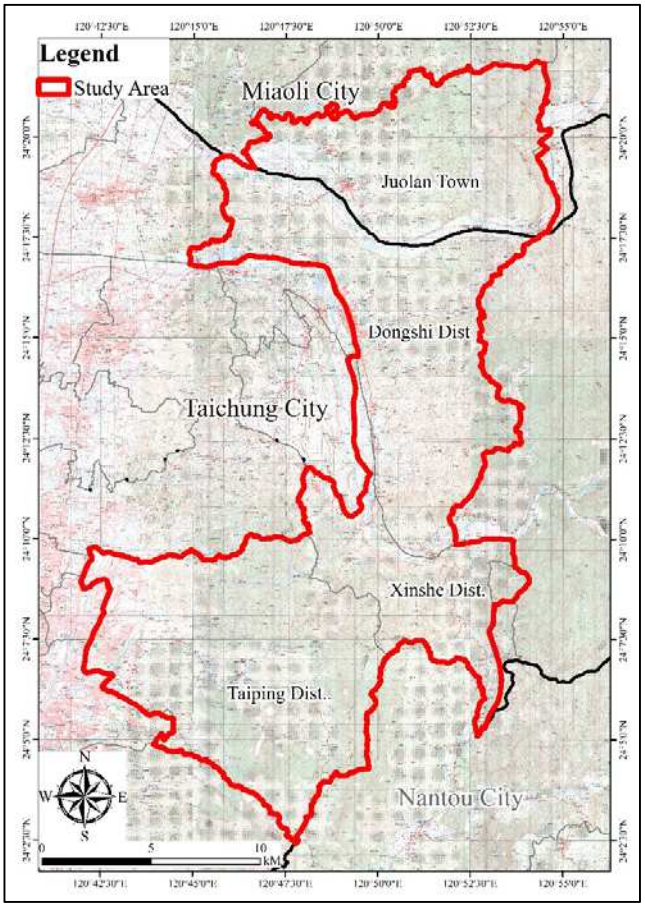

Figure 1. Location of the study area on topographic map. (NLSM, 2000)

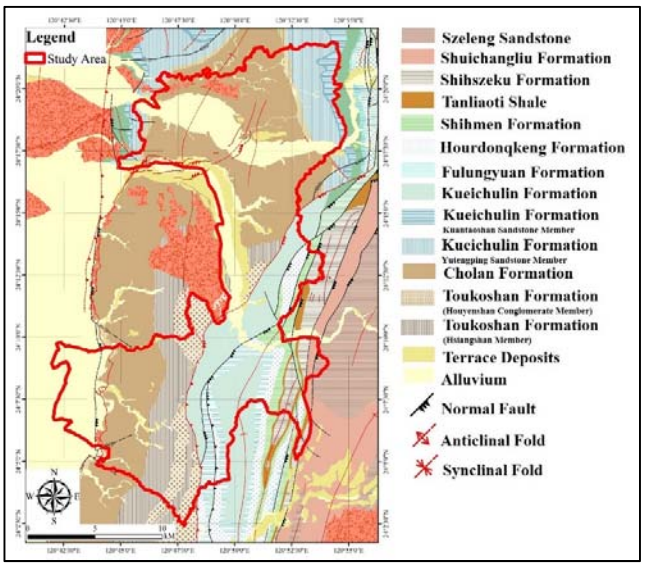

Figure 2. The geological map of the study area. (CGS, 2013)

sandstone and shale, and Cholan Formation, which is interbedded sandstone, mudstone and shale. Parts of Toukoshan Formation, Fulungyuan Formation, Hourdonqkeng Formation, and Shihmen Formation

are also found, which are conglomerate, sandstone and shale, siltstone and shale, and thickly bedded sandstone, shale, and/or with thin alternations, intercalated with fossil-rich layers, respectively. The shallow landslides have been defined by different researchers (Van Asch et al.1999, Khazai and Sitar, 2000, Santacana et al. 2003), and are typically defined as a small scale sliding with a depth of few meters which often occurred in soil or weathered rock layer. Central Geology Survey (CGS) (CGS, 2011) had conducted mapping of the landslides since 2010 after typhoon Morakot, 2009, which caused extensive landslide hazard in Taiwan. The landslide mapping was executed using aerial photos and FORMOSAT II satellite images taken after 2010, and the mapped results were validated with some field investigations. The landslide scars were manually interpreted with criteria of: long strips with light tones on aerial photographs showing shallow grooves, uncoordinated plant tones with the surrounding area, and toe area is flat with accumulation related to landslides. The mapping criteria excluded slopes with slope angle larger than 55˚, which were speculated to be of the rock/soil fall type of failure, and the threshold slope height was set at 5m and threshold area was 20 × 20 meters based on 5m resolution digital terrain model (DTM) (CGS, 2010). The mapped landslide scars included different types of ground erosions and landslides, and firstly the riverbank erosions were excluded from the mapped scars. Further edition of mapped landslides was conducted by overlapping landslide scars with the deep-seated landslide inventory provided by the National Science and Technology Center for Disaster Reduction (https://dmap.ncdr.nat.gov.tw/) to eliminate scars of the deep-seated landslides. A total of 1191 landslide scars remained and were considered as the scars caused by shallow landslides. A close examination of these scars shows characteristics of small scale sliding with shallow depth as proposed by several researches (Van Asch et al.1999, Khazai and Sitar, 2000, Santacana et al. 2003).

3 INVENTORY OF SHALLOW LANDSLIDE AND ANALYSIS UNIT

In order to prepare the attributes of geomorphologic properties of the causal factors, the landslide scars were examined. It was found that most of the areas of the landslide scars were smaller than 0.5 Hectare, and distribution of the area of landslide scars was as shown in Figure 3. About 53.6% of the landslide scar had an area ranging from 400 to 2000 m^2 in Figure 3. Lin, et al. (2017a) made a comparison between the distribution of landslide area and that of the typical slope unit often used in the landslide susceptibility analysis. It was found that most of the shallow landslides had a much smaller area compared to the area of a typical slope unit, and to use the slope unit for susceptibility analysis would lead to over estimation of the analysis results, and this was also recognized by other researchers (Reichenbach, et al. 2018). Thus, the grid unit was used in this study with the 5 m resolution DTM produced in 2003. To generate the related geomorphologic parameters for each landslide scar properly, typically the grids of 3 × 3 were used in the Geographical Information System (GIS), and thus a threshold landslide area was set at 20 × 20 m, which also consisted with the mapping threshold area criterion. Figure 4 showed the resulting landslide distribution for the analysis. In addition, due to the vast number of grids in the study area and a close relation of triggering debris flow by the shallow landslides, the debris flow torrent basins (Soil and Water Conservation Bureau, 2019) in the study area were selected and the basin-wise grids were used. The debris flow torrent basins distributed relatively uniformly in the study area in Figure 4, and grids in the basins were used for construction and validation of the landslide susceptibility assessment model.

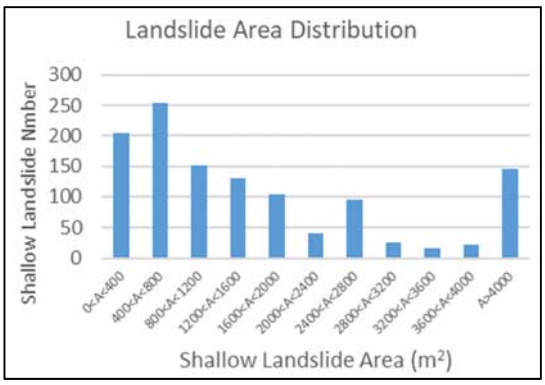

Figure 3. Distribution of the landslide scar areas.

When mapping the landslide scar with aerial photos or satellite images, the scar often contained both the head scarp area and the down slope deposition area. Therefore, the mapped scars might include a larger landslide area than the actual landslide area with part of deposition area included. Field investigation conducted during mapping

work also confirmed this situation as illustrated by Figure 5 (Lin, et al., 2017a). In Figure 5, the field

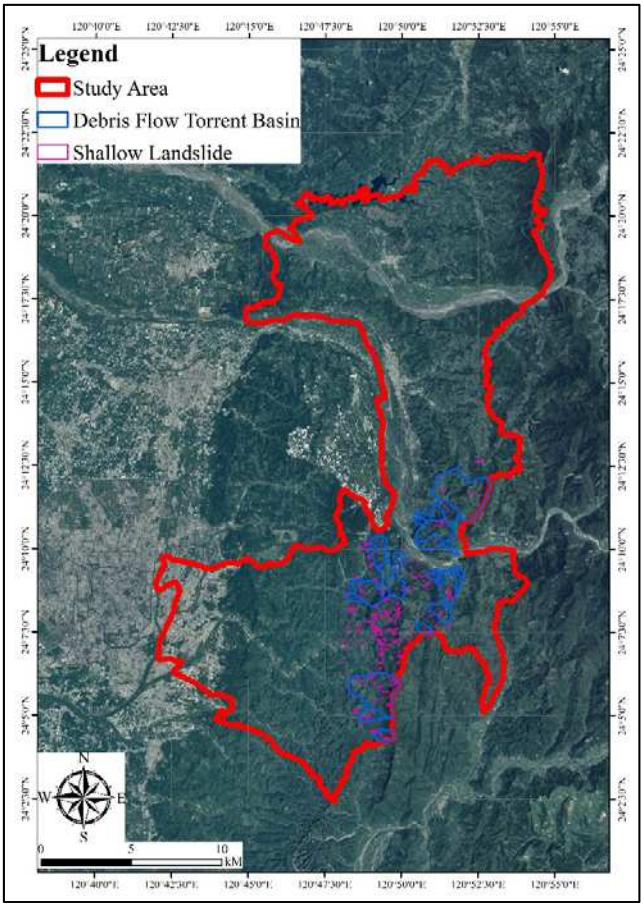

Figure 4. Landslide distribution and debris flow torrent basins used in this study.

conditions of the upper slope distinctly showed the scarp and sliding surface of the slope, while the lower part condition of the slope was not clear due to the deposition mass on the lower part of slope. A set of topographic analysis was conducted using Light Detecting and Ranging technique (LiDAR) derived high resolution DTM on typical mapped cases before and after the shallow landslide. Results of topographic variation of two typical shallow landslide cases were illustrated in Figure 6 (Lin & Wang, 2018). In the two cases, approximately upper half of the slope suggested subsidence after the landslides, while the lower half showing deposition or being elevated. Thus the upper part provided more information of the landslide characteristics, while the condition of the lower half was unclear. Thus only the upper half of the mapped scars were adopted as landslide unit in the susceptibility analysis to avoid uncertainties caused by possible deposition area of the lower half scar.

Figure 5. Illustration of field conditions of a typical shallow landslide in Kaohsiung City, south Taiwan. (Lin, et al. 2017a)

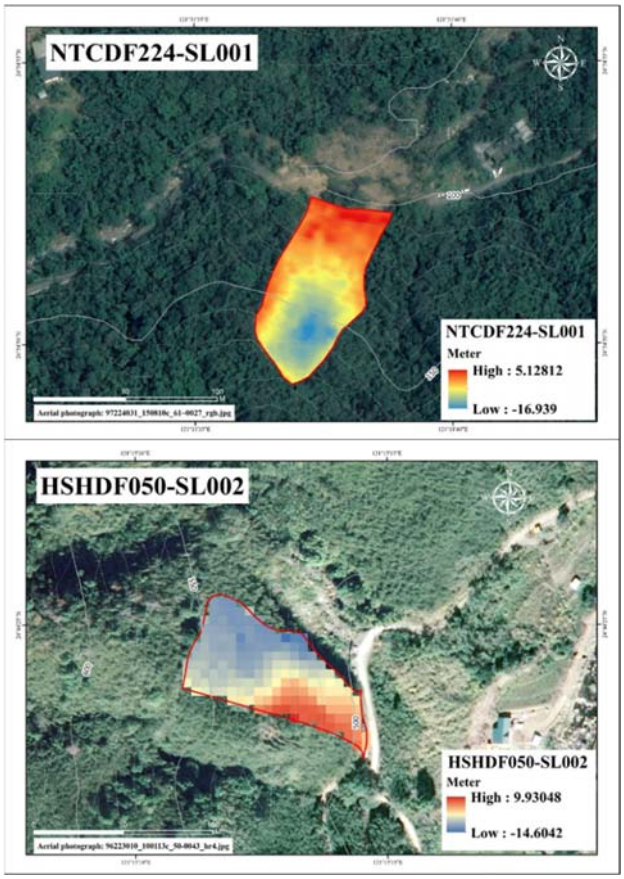

Figure 6. Illustration of topographic variations of two shallow landslides in Nantou County (upper) and Hsinchu County (lower). (Lin & Wang, 2018)

4 CAUSAL FACTOR AND DISCRIMINANT ANALYSIS

The discriminant analysis is one of the statistical methods often used to discriminate between two different classes (landslide and non-landslide

groups), and to construct landslide susceptibility map accordingly (Guzzetti, et al. 1999, Reichenbach, et al. 2018). This study utilized a discriminant function to discriminate between the landslide units and the non-landslide units. The landslide units (taken as 1) were taken as the units in the upper half of the mapped scars in the debris flow torrent basins as discussed in the previous section, and the units outside the mapped scar were considered as non-landslide units (taken as 0). The discriminant function is a linear combination of multiple factors with coefficients implying weighting of each factor. The factors in the linear relation represent characteristics of the shallow landslide that could effectively discriminate the two groups. Preliminary causal factors were selected referring to previous researches (Carrara, et al., 1991, Guzzetti, et al. 1999, Lin, et al., 2017a, Reichenbach, et al. 2018, Huang, 2019), which included slope angle, slope aspect, elevation, horizontal profile curvature, vertical profile curvature, lithology, distance to geological structure, distance to river, and distance to road.

The factors composed mainly of the geological and geomorphological characteristics of each unit. For the categorical type factors such as lithology and aspect, the landslide ratio was used to represent effect of the specific factor. All factors need to fulfill the requirements of normal distribution, significance, and independency for the discriminant analysis. However, when the number of data is large, the normal distribution can be assumed to be valid such as in this study.

The independency of the factors was examined using the Pearson correlation coefficient of covariance. The factor was considered as independent when the absolute value of correlation coefficients with respect to other factors being smaller than 0.2. Each causal factor was then normalized by subtracting its mean value and divided by the standard deviation so that the distribution value of all factors will range mainly from -1 to 1 with a mean value of 0 (Lin, 2008). Thus, the coefficient of each factor in the discriminant function could provide the true weighting of that specific factor. The significance of each factor was evaluated using the area under the receiver operating characteristic curve (AUC) when adopted in the discriminant function. The receiver operating characteristic curve was a curve plotted as true positive rate versus false positive rate. Factor yielding an AUC larger than 0.5 was considered as significant for discrimination between the two groups with the larger the AUC value the higher the significance. The causal factors satisfying all the criteria were distance to road, lithology, slope angle, aspect, distance to geological structure, and vertical profile curvature in the order of decreasing AUC values as listed in Table 1. However, the AUC of the vertical profile curvature was only slightly larger than 0.5, and might not be so significant for discrimination of the two groups.

Table 1. Significance of causal factors in terms of calculated AUC

Causal factor	Slope angle	Distance to road	Aspect	Vertical profile curvature	Litho-logy	Distance to geological structure
AUC	0.618	0.632	0.6	0.512	0.627	0.559

5 SUSCEPTIBILITY ASSESSMENT MODEL AND VALIDATION

To construct the susceptibility model of the study area, random sampling of the landslide grids and non-landslide grids was adopted (Chuang, 2010). Approximately one half of the landslide units were sampled and about the equivalent number of non-landslide units were sampled for construction of the model. The other half of the landslide units and about same number of non-landslide units were then adopted for validation of the fitted model. The resulting fitted discriminant model of the study area is as listed below:

$$Z = (0.564 \times Z_{slope}) + (0.238 \times Z_{aspect}) + (-0.022 \times Z_{profile}) + (0.59 \times Z_{road}) + (-0.054 \times Z_{geologic\ structure}) + (0.671 \times Z_{lithology}) - 0.413 \quad (1)$$

where Z is the discriminant functon Z score, and Z_{slope}, Z_{aspect}, $Z_{lithology}$, $Z_{proilfe}$, Z_{road}, $Z_{geologic\ structure}$ are the causal factor of slope angle, aspect, lithology, vertical profile curvature, distance to road, and distance to geological structure, respectively. It can be observed that the lithology factor had the highest coefficient in Eq. (1), implying being the most significant factor and followed by distance to road, slope angle, and slope aspect. The coefficients of distance to geological structure and vertical profile curvature factors appeared to be not so significant as already suggested by the AUC values in Table 1. Noted that the order of significance following the values of weighting coefficient is slightly different from AUC values directly. Still, lithology , distance to road, slope angle, and aspect are the major

contributing factors as in Table 1.The discriminant function *Z* scores of the validation group units were then calculated using Eq. (1) to provide validation of the fitted model. The accuracy is defined as the percentage of either landslide units or non-landslide units being identified correctly, and the overall accuracy was defined as the percentage of all units correctly identified. The results of both the fitting units and validation units were as listed in Table 2. In Table 2, the overall accuracy of the fitting group was about 71.2%, while the validation group also had an equivalent accuracy of 71%. Both groups showed about the same accuracy for discriminating landslide from non-landslide units, which suggeted robustness of the assessment model. The susceptibility map was then developed using the calculated discriminant function *Z* score values as shown in Figure 7, by taking *Z* score value smaller than discriminant value as with low susceptibility (in green color). The higher score suggested a higher susceptibility. It can be observed that most of the mapped landslide scars situated in the moderate to high susceptibility zone in Figure 7, and the assessment model appeared to provide satisfactory results.

The backward prediction was conducted to further validate the assessment model and susceptibility map. The landslide historical inventory by the CGS before typhoon Morakot, 2009 was adopted (CGS, 2007, 2008). The mapping of landslides was conducted using satellite images and aerial photos but not with as strict criteria as adopted for inventory used for establishing the assessment model. The accuracy of the historical inventory calculated using Eq. (1) was listed in Table 3 with the accuracy for the landslide units of 74.7% and the non-landslide units of 65%. The accuracy was about equivalent to the accuracy of the study group with that of the landslide group slightly higher than the study group. The accuracy of non-landslide units was lower than the study group, it might be due to the large number and extensive distribution of the non-landslide units. In addition, the historical inventory did not follow a strict mapping criterion. The good and consistent accuracy of the landslide units also suggested that the definition of the landslide unit was appropriate, and could achieved consistent results. The historical landslide inventory was plotted on the susceptibility map in Figure 8. It can be observed that most of the historical landslide scars were with moderate to high susceptibility and appeared to consist well with the susceptibility assessment results.

Table 2 Percentage accuracy of the fitting versus the validation groups for the susceptibility model

Study group estimation, %		Assessment model	
		landslide	non-landslide
Fitting group	landslide	72.2	27.8
	non-landslide	29.8	70.2
Validation group	landslide	72.8	27.2
	non-landslide	30.8	69.2

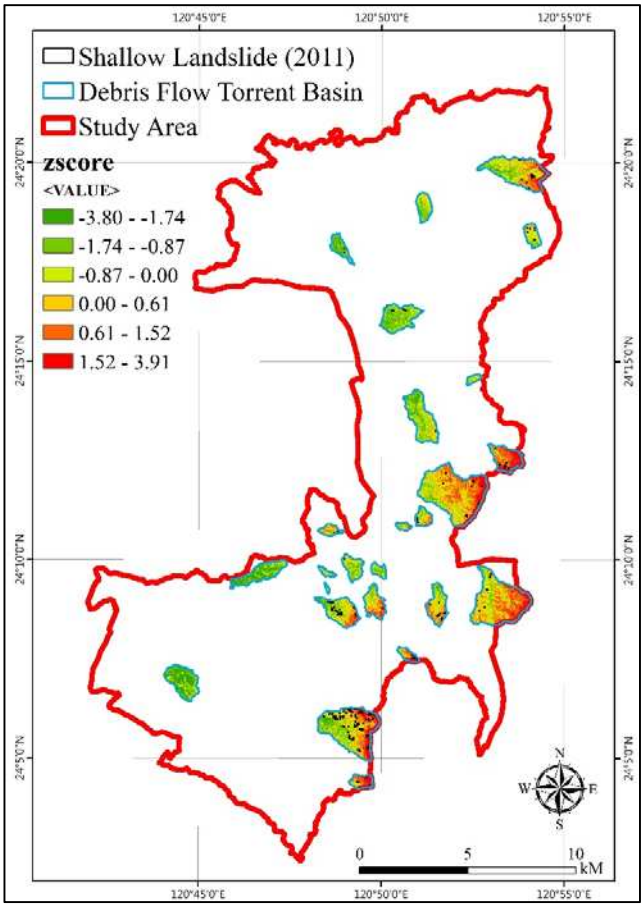

Figure 7. Shallow landslide susceptibility map based on *Z* score values of the study area.

Table 3 Percentage accuracy of the historical inventory using the susceptibility assessment model

Study group estimation, %		Assessment model	
		landslide	non-landslide
Historical inventory	landslide	74.7	25.3
	non-landslide	35.0	65.0

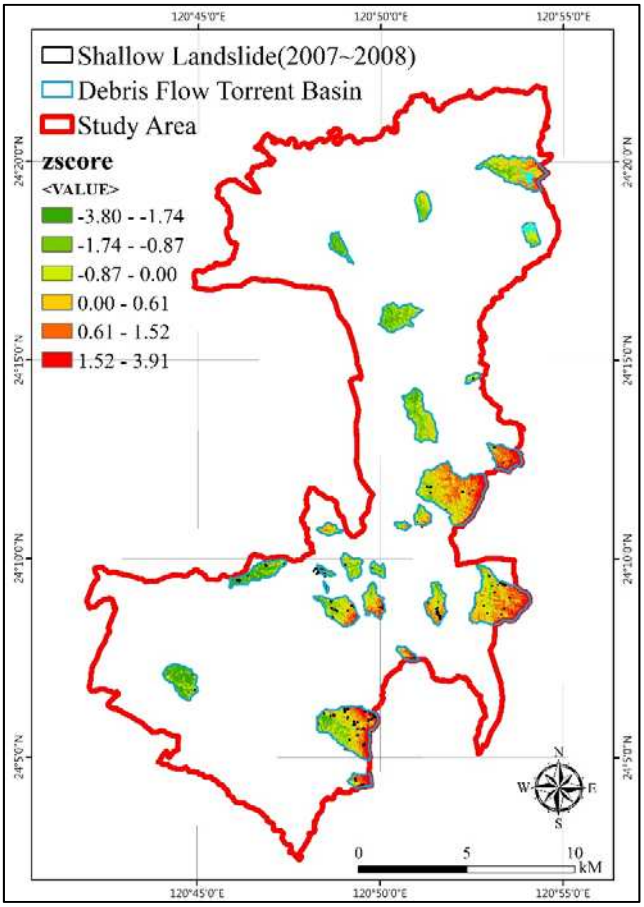

Figure 8. Susceptibility map with historical shallow landslide inventory.

6 CONCLUSION

In this research, the susceptibility analysis was conducted for the study area in central Taiwan. Landslide scars mapped using aerial photos and satellite images after typhoon Morakot, 2009, were used. The inventory was screened to eliminate ground erosions different from shallow landslide, and then edited by threshold area considering the grid size of analysis unit. The causal factors were selected and examined to satisfy the requirements of independency and significance and used in the discriminant analysis for assessment of shallow landslide susceptibility. Randomly sampled landslide units and non-landslide units were used to construct susceptibility model, which was then validated with a separate group of data. Both the fitting and validation data groups provided consistent accuracy and satisfactory results. A backward prediction was also conducted using the historical inventory data, and a comparable accuracy was achieved, which suggested the robustness of the susceptibility assessment model.

7 ACKNOWLEDGEMENT

This research was supported by the Soil and Water Conservation Bureau, project number: SWCB-108-228.

8 REFERENCES

Carrara, A., Cardinali, M., Guzzetti, F. and Reichenbach, P. (1991). "*Gis Technology in Mapping Landslide Hazard*". Geographical Information Systems in Assessing Natural Hazards, 135-175.

Central Geological Survey. (2007). "*Geological investigation and database for upstream watershed of flood-prone area*". Taipei, Taiwan.

Central Geological Survey. (2008). "*Geological investigation and database for upstream watershed of flood-prone area*". Central Geological Survey, Ministry of Economic Affairs.

Central Geological Survey. (2011). "*Analysis of geological sensitive properties of hazardous area by typhoon Morakot*". Taipei, Taiwan, 266p. 99-5826901000-7-D3-01.

Central Geological Survey. (2013). "*Geological investigation and database for upstream watershed of flood-prone area*". Central Geological Survey, Ministry of Economic Affairs.

Chuang, H. H. (2012), "*Potential analysis of debris flow torrents considering spatial and rainfall variations*". Thesis, National Taiwan University.

Guzzetti, F, Carrara, A., Cardinal, M., and Reichenbach, P. (1999) "*Landslide hazard evaluation: a review of current techniques and their application in a multi-scale study, Central Italy*", Geomorphology, 31: 181–216

Harp, E., Michael, J., and Laprade, W. (2006), "*Shallow-landslide hazard map of Seattle, Washington*", USGS

Huang, P. H. (2019). "*Assessment of shallow landslide susceptibility using the random forest algorithm*". Thesis, National Taiwan University.

Khazai, B., and Sitar, N. (2000), "*Assessment of seismic slope stability using GIS modeling*". Geographic Information Sciences, Vol.5, No. 2, 121-128.

Lin, Y. X. (2008). "*Potential of analysis of debris flow: fitting and prediction of discriminant analysis*". Thesis, National Taiwan University.

Lin, M. L., Chen, T. C., Wang, K. L., Chen, Y. S., Su, C. Y., Chuang, H. H. (2014). "*Discriminant method of different types of landslide and the sediment transportation analysis in Liouguei-Baolai area*". Soil and Water Conservation Bureau.

Lin, M. L., Chen, T. C., Wang, K. L. (2017a). "*Shallow landslide disaster prevention management planning and research*". Soil and Water Conservation Bureau.

Lin, M.L., Lin, S.C., and Lin, Y.C. (2017b), "*Review of landslide occurrences and climate change in Taiwan*", Slope safety preparedness for impact of climate change, 409-435

Lin, M. L., and Wang, K. L. (2018). "*Investigation and delineation of the affected area of shallow landslide and preliminary assessment of settlement hazard*". Soil and Water Conservation Bureau.

National Science and Technology Center for Disaster Reduction, Disaster Potential Map, Site: *https://dmap.ncdr.nat.gov.tw/.*

National Land Surveying and Mapping Center. (2000), "*1/25,000 topographic map, 3rdEd*", Ministry of Interior.

Reichenbach, P., Rossia, M., Malamud, B.D., Mihir, M., and Guzzetti, F. (2018). *"A review of statistically-based landslide susceptibility models".* Earth-Science Reviews 180: 60-91.

Santacana, N., Baeza, B., Corominas, J., Depaz, A., and Marturia, J. (2003) "*A GIS-Based nultivariate statistical analysis for shallow landslide susceptibility mapping in La Pobla de Lillet area (Eastern Pyrenees, Spain)*", Natural Hazards 30: 281–295

Soil and Water Conservation Bureau -Debris Flow Disaster Prevention Information. (2019), Site: *https://246.swcb.gov.tw/.*

Van Asch, Th.W.J., Buma, J., Van Beek, L.P.H. (1999), *"A view on some hydrological triggering systems in landslides"*, Geomorphology, 30: 25–32

The Authors declares that they do not have Conflict of Interest with the contents and authorize the Editorial Committee of XIII ISL to publish the paper during the next two years, according of Authors Instructions.